

# The effect of holmium doping on the magnetic and transport properties of $\text{La}_{0.7-x}\text{Ho}_x\text{Sr}_{0.3}\text{MnO}_3$ ( $0 \leq x \leq 0.4$ )

P Raychaudhuri<sup>†</sup>, T K Nath, P Sinha<sup>‡</sup>, C Mitra, A K Nigam, S K Dhar and R Pinto

Tata Institute of Fundamental Research, Homi Bhabha Road, Colaba, Mumbai-400 005, India

Received 11 August 1997

**Abstract.** We have studied the evolution of the transport and magnetic properties with holmium doping for  $\text{La}_{0.7-x}\text{Ho}_x\text{Sr}_{0.3}\text{MnO}_3$  ( $0 \leq x \leq 0.4$ ). We observe a systematic decrease in the ferromagnetic transition temperature ( $T_c$ ), the metal–insulator transition temperature ( $T_p$ ) and the rhombohedral cell volume with increasing holmium concentration. For the concentration with  $x = 0.4$ , we observe a metallic spin-glass phase with the spin-glass freezing temperature  $T_{cusp} \sim 50$  K, and a large magnetoresistance ratio at low temperature, which indicates that a proportion of the spins are in a frustrated state. The high-field magnetization of the holmium-doped samples is much less than the magnetization that would be expected if the  $\text{Mn}^{3+}/\text{Mn}^{4+}$  were in a ferromagnetic state, showing that there is substantial canting in the manganese lattice. We believe that the ferromagnetic component in the spin-glass phase for  $x = 0.4$  crosses the percolation threshold, giving rise to metallicity in the sample.

## 1. Introduction

Recent studies on  $\text{R}_{1-x}\text{M}_x\text{MnO}_3$  ( $\text{R} = \text{rare earth}$ ,  $\text{M} = \text{Ca, Sr}$ ) perovskite oxides exhibiting colossal magnetoresistance have revealed many interesting properties of these materials. It has been observed that the magnetic and transport properties of these oxides are strongly dependent on the size of the cation R/M. With decreasing average ionic radius at the cation site, the metal–insulator transition temperature ( $T_p$ ) and the ferromagnetic transition temperature ( $T_c$ ) shift to lower temperature with increase in the magnetoresistance close to the metal–insulator transition temperature [1, 2]. More recently De Teresa *et al* [3] observed from magnetic and neutron diffraction studies that with increasing Tb doping at the lanthanum site in  $(\text{LaTb})_{2/3}\text{Ca}_{1/3}\text{MnO}_3$ , the material goes into an insulating spin-glass state. Similar insulating spin-glass states have been observed in  $\text{Pr}_{0.7}\text{Ca}_{0.3}\text{MnO}_3$  and  $\text{Eu}_{0.58}\text{Sr}_{0.42}\text{MnO}_3$  [4, 5] with the spin-glass freezing temperatures of 95 K and 45 K, respectively. Maignan *et al* [4] have compared the ac susceptibility and dc magnetization data with the neutron diffraction data for  $\text{Pr}_{0.7}\text{Ca}_{0.3-x}\text{Sr}_x\text{MnO}_3$ . There is an apparent contradiction for the  $x = 0$  sample (which has the smallest R/M average ionic radius for these samples) with the magnetization data showing a spin-glass-like behaviour below the cusp temperature ( $T_{cusp}$ ) whereas the neutron diffraction data [6, 7] show evidence of a ferromagnetic component developing below  $T_{cusp}$ . However, the total magnetic moment calculated for the manganese from neutron studies is smaller than the expected spin-only

<sup>†</sup> E-mail: pratap@tifrc3.tifr.res.in.

<sup>‡</sup> Present address: Indian Institute of Technology, Delhi, India.

value for manganese, showing that not all of the spins contribute to the ferromagnetic ordering. These results call for closer investigation of the evolution of the magnetic and transport properties when smaller rare earths are substituted at the lanthanum site in  $\text{La}_{1-x}\text{Sr}_x\text{MnO}_3$ .

In this work, we report the magnetic and transport properties of  $\text{La}_{0.7-x}\text{Ho}_x\text{Sr}_{0.3}\text{MnO}_3$  ( $0 \leq x \leq 0.4$ ). Contrary to earlier reports on similar manganite spin-glass samples [3–5] where the spin-glass phases were insulating, we observe here a metallic spin-glass phase for  $x = 0.4$  suggesting that ferromagnetic correlations persist in the frustrated region. This is consistent with the neutron diffraction result at zero field for the similar spin-glass sample  $\text{Pr}_{0.7}\text{Ca}_{0.3}\text{MnO}_3$  where a ferromagnetic component appears below  $T_{cusp}$ . There is a gradual increase in the spin-glass-like behaviour when the holmium concentration ( $x = 0.3$  and  $0.4$ ) in the sample is increased, showing that the transition to the spin-glass phase might be a gradual one with increasing number of spins going to a frustrated state. The magnetization at high field for the holmium-doped samples is much less than the value that would be expected if the manganese lattice was in a ferromagnetic state. This suggests that there is substantial canting in the manganese sublattice which is responsible for the large increase in resistance in these samples.

## 2. Experimental details

The samples were prepared through a solid-state reaction route by mixing stoichiometric compositions of  $\text{La}_2\text{O}_3$ ,  $\text{Ho}_2\text{O}_3$ ,  $\text{SrCO}_3$  and  $\text{MnO}_2$  with purity not less than 99.99%. The oxides were mixed for few hours in acetone and calcined at  $1050^\circ\text{C}$  for 24 h. The reacted powder was reground and fired at  $1050^\circ\text{C}$  for another 24 h, ground again, pelletized, and then the pellets were sintered at  $1550^\circ\text{C}$  in air for 24 h. The temperature was then brought down to  $1000^\circ\text{C}$  and the pellets were subsequently quenched in liquid nitrogen. We observed that this quenching process was essential to obtain a single phase. Samples prepared without quenching showed phase separation into lanthanum-rich and holmium-rich regions in energy-dispersive x-ray analysis (EDX). The samples were characterized through EDX and x-ray diffraction (XRD). The XRD confirmed the single phase for all of the compositions. The EDX composition was always within 2% of the nominal composition.

The magnetization was measured as a function of temperature and field using either a Quantum Design SQUID magnetometer or by the Faraday method. The resistance and magnetoresistance up to 40 kOe were measured using the conventional four-probe technique from 4.2 K to room temperature using a superconducting magnet.

**Table 1.** Lattice parameters,  $T_c$  and  $T_p$  for  $\text{La}_{0.7-x}\text{Ho}_x\text{Sr}_{0.3}\text{MnO}_3$ .

$\text{La}_{0.7-x}\text{Ho}_x\text{Sr}_{0.3}\text{MnO}_3$ $x$	Lattice parameters		Cell volume ( $\text{\AA}^3$ )	$T_c/T_{cusp}$ (K)	$T_p$ (K)
	$a$ ( $\text{\AA}$ )	$\alpha$ (deg)			
0.05	5.482	60.442	117.70	$T_c > 310$	$> 310$
0.1	5.493	60.185	117.72	$T_c = 304$	300
0.2	5.464	60.140	115.76	$T_c = 220$	218
0.3	5.467	59.957	115.64	$T_c = 162$	145
0.4	5.456	59.988	114.85	$T_{cusp} = 50$	98

### 3. Results and discussion

#### 3.1. Magnetic studies

The XRD showed all the compositions to have the  $\text{La}_{0.7}\text{Sr}_{0.3}\text{MnO}_3$ -type structure ( $R\bar{3}c$ ), without the presence of any impurity phase. The lattice constants  $a$ ,  $\alpha$  and the cell volume for the rhombohedral cell are shown in table 1. There is a gradual decrease in the lattice parameter and the cell volume with increasing holmium concentration for all of the compositions above  $x = 0.1$ . The metal-insulator transition temperature ( $T_p$ ) and the ferromagnetic transition temperature ( $T_c$ ) or spin-glass freezing temperature ( $T_{cusp}$ ) are also shown in the same table. There is a decrease in  $T_c$  and  $T_p$  with the increasing holmium concentration. The decrease in the average ionic size of the cation results in a decrease of the perovskite tolerance factor which results in the distortion of the  $\text{MnO}_6$  octahedra. Thus the Mn–O–Mn bond angle deviates from the ideal  $180^\circ$ . Since the double exchange [8] between  $\text{Mn}^{3+}$  and  $\text{Mn}^{4+}$  is strongly dependent on the Mn–O–Mn bond angle through the matrix element  $t_{ij}$ , this results in a narrowing of the  $e_g$  bandwidth which in turn results in the reduction of the hopping probability of the electron between the neighbouring  $\text{Mn}^{3+}/\text{Mn}^{4+}$  ions. This reduction in the hopping probability  $t_{ij}$  is corroborated by the decrease in  $T_c$  and  $T_p$ .

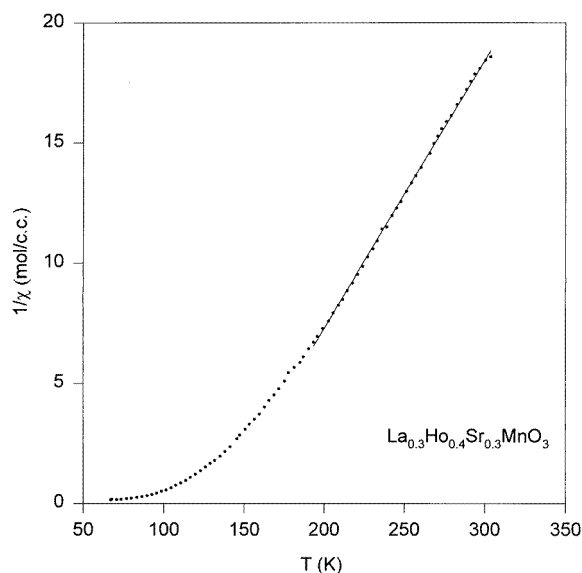


**Figure 1.**  $1/\chi$  versus  $T$  for  $\text{La}_{0.3}\text{Ho}_{0.4}\text{Sr}_{0.3}\text{MnO}_3$  measured at 600 Oe. The solid line shows the fit to the linear portion of the curve.

Figure 1 shows the susceptibility ( $\chi^{-1}$ ) as a function of temperature ( $T$ ) for the sample with  $x = 0.4$  which has the lowest magnetic transition temperature measured at 500 Oe. There is a deviation from the Curie–Weiss behaviour below  $T = 190$  K though for this composition the spin-glass freezing temperature ( $T_{cusp}$ ) is 50 K. This deviation from the Curie–Weiss behaviour much before the cusp temperature is reached is typical of spin-glass systems [9]. The Curie constant ( $C$ ) obtained from the  $\chi^{-1}$ – $T$  data by fitting a linear curve in the temperature interval 195 K to 300 K was  $8.98 \text{ emu K Oe}^{-1} \text{ mol}^{-1}$ . The effective Bohr magneton number for  $\text{Ho}^{3+}$  ( $p_{eff(\text{Ho})}$ ) was calculated from the Curie constant by

subtracting the contribution coming from  $\text{Mn}^{3+}$  and  $\text{Mn}^{4+}$  (assuming  $\text{Mn}^{3+}/\text{Mn}^{4+}$  to be in the stoichiometric ratio 70%/30%) using the formula

$$(p_{eff})^2 = 0.3g^2S_{\text{Mn}(4+)}(S_{\text{Mn}(4+)} + 1) + 0.7g^2S_{\text{Mn}(3+)}(S_{\text{Mn}(3+)} + 1) + 0.4g_{\text{Ho}}^2(p_{eff(\text{Ho})})^2 \quad (1)$$

where  $(p_{eff})^2$  is given by

$$(p_{eff})^2 = 3Ck/N\mu_B^2$$

and where  $g$  ( $=2$ ) and  $g_{\text{Ho}}$  stand for the gyromagnetic ratio of the manganese ions and holmium ions respectively,  $S_{\text{Mn}(4+)}$  and  $S_{\text{Mn}(3+)}$  stand for the total spin quantum numbers for  $\text{Mn}^{4+}$  and  $\text{Mn}^{3+}$  respectively,  $k$  is the Boltzmann constant,  $N$  is the Avogadro number and  $\mu_B$  stands for the Bohr magneton. The experimental value obtained for  $p_{eff(\text{Ho})}$  was 11.2 which is close to the theoretical value of 10.6 for the free  $\text{Ho}^{3+}$  ion. The slight increase over the free-ion estimate could occur because of the fact that when subtracting the manganese contribution all the manganese ions are treated in the localized model which might not be a correct description for the manganese  $e_g$  electrons.

Figures 2(a) and 2(b) show the magnetization versus temperature ( $M-T$ ) curve at 4 kOe, 15 kOe and 50 kOe for the samples with  $x = 0.2$  and 0.3. At low temperatures there is a departure from the normal ferromagnetic behaviour with the  $M-T$  curve showing an increasing trend. This increase is less pronounced for samples with smaller holmium concentration and is, therefore, associated with the holmium paramagnetic moments. This increase is also absent when the magnetization is measured at lower fields. Figure 2(c) shows the temperature dependence of the magnetization of the sample with  $x = 0.3$  taken at 600 Oe which is typical of a normal ferromagnet. With increasing field the departure from the normal behaviour becomes pronounced with the magnetization increasing at low temperature. This is natural since at low fields the ratio of the magnetization of the ferromagnetic manganese to that of the paramagnetic holmium is much larger than at high fields. To get a quantitative feeling for this we can compare the ratio of the magnetization of  $\text{La}_{0.7}\text{Sr}_{0.3}\text{MnO}_3$  (where the magnetization is from the manganese alone) with the paramagnetic magnetization of holmium calculated from the usual expression

$$M = N\mu = NJg\mu_B F(J, y) \quad (2)$$

where  $y = Jg\mu_B H/k_B T$ ,  $J = 8$ ,  $H$  is the external magnetic field,  $M$  is the magnetization per mole of holmium,  $N$  is the Avogadro number and  $F(J, y)$  is the usual Brillouin function defined by

$$F(J, y) = (1 + 1/2J)\coth[(1 + 1/2J)y] - (1/2J)\coth(y/2J).$$

This ratio of the average magnetic moment of ferromagnetic manganese to that of paramagnetic holmium is 17.05 at 600 Oe and 2.06 at 15 kOe. Figure 3(a) shows the field ( $H$ ) dependence of  $M$  for various samples taken at 5 K plotted in units of Bohr magneton ( $\mu_B$ ) per formula unit. The saturation magnetization of the  $\text{La}_{0.7}\text{Sr}_{0.3}\text{MnO}_3$  sample is  $3.8 \mu_B$  which is very close to the theoretical value  $3.7 \mu_B$  calculated from the nominal  $\text{Mn}^{3+}/\text{Mn}^{4+}$  ratio. For higher holmium concentration ( $x \geq 0.2$ ) the magnetization does not saturate up to 55 kOe. In order to investigate the effect of holmium doping we subtracted the magnetization of  $\text{La}_{0.7}\text{Sr}_{0.3}\text{MnO}_3$  ( $M_{x=0}$ ) from the magnetization of the samples with various levels of holmium doping ( $M_x$ ). The  $M_x - M_{x=0}$  versus  $H$  curves for various values of  $x$  are shown in figure 3(b). There is a rapid increase followed by a decrease below the technical saturation coming presumably from domain reorientation at low field for all of the samples except the one with  $x = 0.4$ . Above technical saturation the curve is always

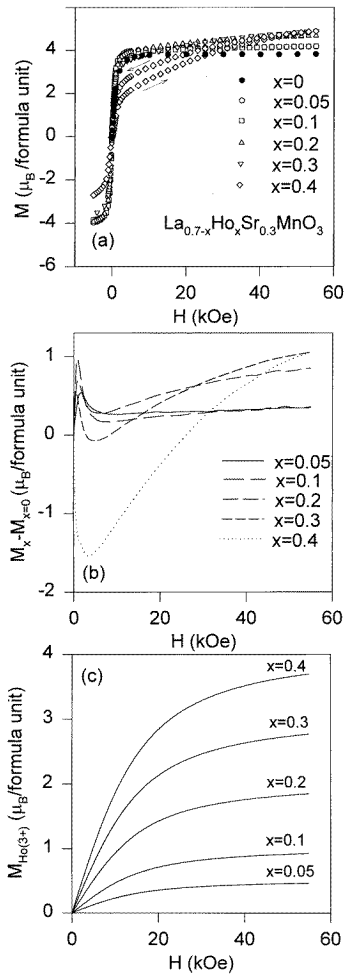
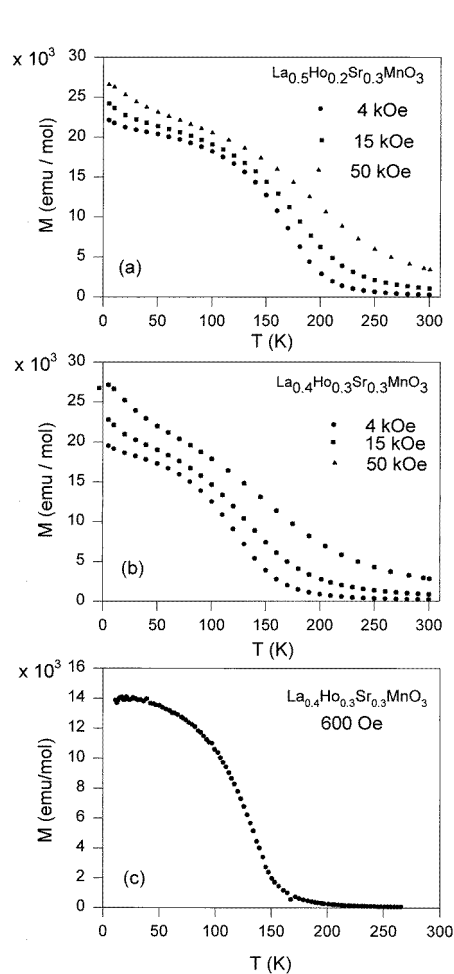


**Figure 2.** The magnetization ( $M$ ) versus the temperature ( $T$ ) at 4 kOe, 15 kOe and 50 kOe for (a)  $x = 0.2$  and (b)  $x = 0.3$ ; (c) the magnetization versus the temperature for  $x = 0.3$  at 600 Oe.

**Figure 3.** (a) The magnetization ( $M$ ) as a function of field ( $H$ ) up to 55 kOe for various values of  $x$  at 5 K; (b)  $M_x - M_{x=0}$  as a function of field for various values of  $x$ ; (c) the magnetization contribution of paramagnetic  $\text{Ho}^{3+}$  per formula unit for various values of  $x$ .

positive for  $x = 0.05, 0.1$  and  $0.2$ , showing that the magnetization is larger than that of  $\text{La}_{0.7}\text{Sr}_{0.3}\text{MnO}_3$  at all fields. For  $x = 0.4$  the curve decreases rapidly from zero at low fields, and this is followed by a steady increase. This behaviour for the  $x = 0.4$  sample is related to the spin-glass nature of this sample, where the low-field behaviour is governed by the interactions between spin clusters. Similar behaviour is also observed for  $x = 0.3$  where there is a small region of negative value where the magnetization is less than that of the  $\text{La}_{0.7}\text{Sr}_{0.3}\text{MnO}_3$  sample. This could be due to the existence of frustrated spins in the material, though it shows an overall ferromagnetic behaviour. This point is elaborated later. We compared these subtracted curves with the paramagnetic magnetization of  $\text{Ho}^{3+}$  for all of the compositions using equation (2). The latter curves are shown in figure 3(c). It is observed that the contribution of holmium in the subtracted curve at 55 kOe is much less

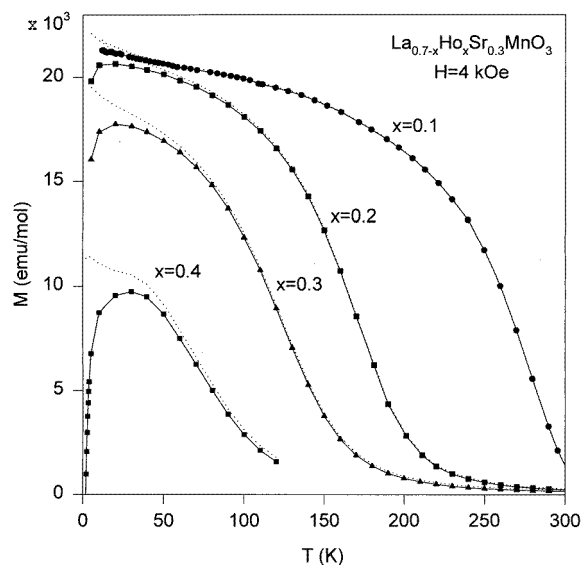


**Figure 4.** The magnetization versus the temperature for various values of  $x$  at 4 kOe after subtracting the paramagnetic holmium contribution. The dashed lines show the curves before subtraction.

than the contribution that would be expected if the  $\text{Ho}^{3+}$  ions were in a paramagnetic state for all of the compositions except for that of the sample with very little doping,  $x = 0.05$ . This shows that there is substantial canting in the manganese lattice when the smaller rare earth holmium is substituted. For the case of very little doping ( $x = 0.05$ ), the canting might be negligible. To understand this point better we have plotted in figure 4 the  $M$ - $T$  curves at 4 kOe after subtracting the paramagnetic holmium contribution for  $x = 0.1, 0.2, 0.3$  and  $0.4$ . The curves for  $x = 0.2, 0.3$  and  $0.4$  show a drop at low temperature indicating that with increasing holmium substitution the manganese sublattice goes into a canted state. This is in accordance with the phase diagram predicted by de Gennes [10] and can be understood as follows. It has been observed from neutron diffraction studies [1] that with the substitution of a smaller rare earth the Mn-O-Mn bond angle changes from the ideal  $180^\circ$ . This results in a reduced double-exchange transfer integral  $t_{ij}$  which is also seen from the reduced  $T_c$ . Since the superexchange interaction is antiferromagnetic, in the presence of superexchange and double exchange the ground state of the system could be a canted state. The canting increases with decrease in the double-exchange/superexchange interaction ratio.

Figures 5(a)-5(c) show the zero-field-cooled (ZFC) and field-cooled (FC) magnetization at 100 Oe for the samples with  $x = 0.2, 0.3$  and  $0.4$ , respectively. The sample with  $x = 0.4$  shows spin-glass behaviour. There is a sharp cusp in the ZFC  $M$ - $T$  curve at 50 K (figure 5(c)). No such cusp is observed in the FC  $M$ - $T$  data. We have measured for comparison the ZFC and FC curves for  $x = 0.2$  (figure 5(a)) and  $x = 0.3$  (figure 5(b)) at 100 Oe. It is seen that there is an increasing thermomagnetic irreversibility with increasing holmium doping. The sample with  $x = 0.3$  shows a drop in the ZFC magnetization at low temperature but does not show a clear cusp. This behaviour is intermediate between that for  $x = 0.2$  and that for  $x = 0.4$ . The behaviour of these samples suggests that the evolution from a ferromagnetic to a spin-glass behaviour is not abrupt but is rather gradual as one increases the concentration of the smaller rare earth, with increasing number of spins going

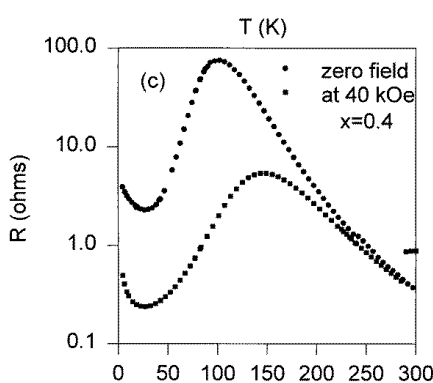
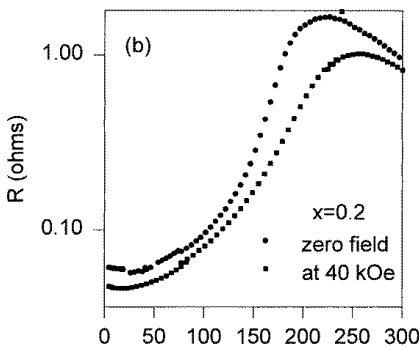
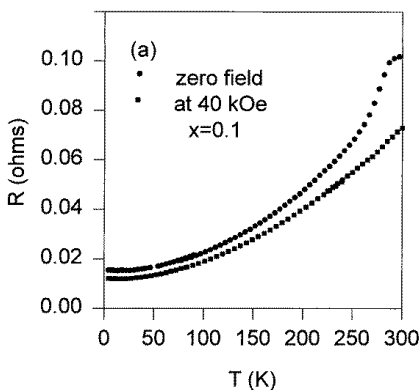
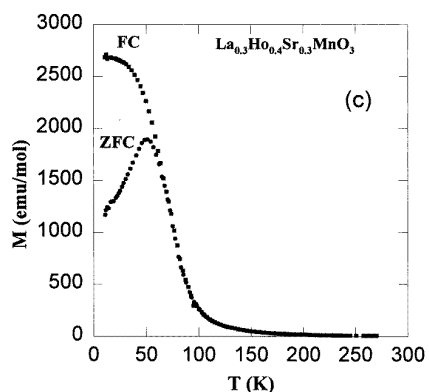
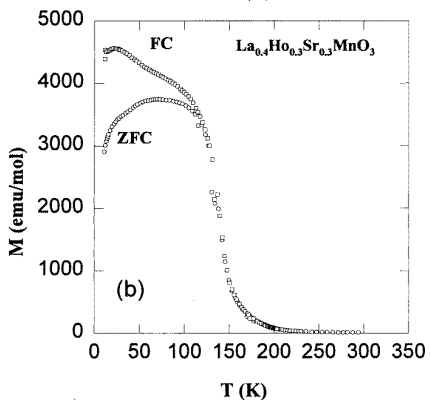
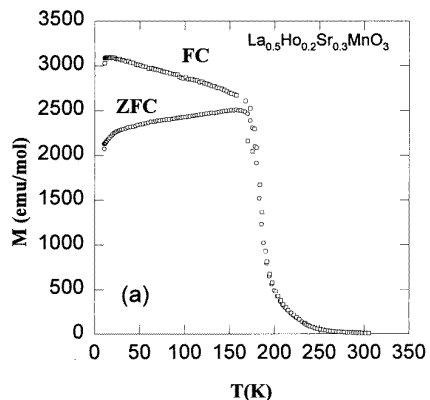


**Figure 5.** ZFC and FC magnetization at 100 Oe for  $x = 0.2, x = 0.3$  and  $x = 0.4$ . The sample with  $x = 0.4$  shows spin-glass behaviour. The behaviour of the sample with  $x = 0.3$  is intermediate between that for  $x = 0.2$  and that for  $x = 0.4$ .

**Figure 6.** The resistance versus the temperature for  $x = 0.1, x = 0.2$  and  $x = 0.4$  samples in zero field and in an applied field of 40 kOe.

into a frustrated state. This observation is consistent with the neutron diffraction studies at zero field on  $Pr_{0.7}Ca_{0.3}MnO_3$  [6, 7] where an unsaturated ferromagnetic component in the magnetization is found to develop below the spin-glass freezing temperature.

## 3.2. Resistivity studies

Figures 6(a)–6(c) show the electrical resistance versus temperature ( $R$ – $T$ ) curve for  $x = 0.1$ , 0.2 and 0.4, respectively. All of the samples show metal–insulator transitions (MIT). The MIT temperature  $T_p$  coincides with  $T_c$  for  $x = 0.1$  and 0.2. For  $x = 0.2$ , there is a small increase in resistivity at low temperatures which corresponds to the drop in magnetization after subtracting the paramagnetic holmium contribution (figure 4). This increase is more pronounced for  $x = 0.4$  where the drop in the holmium-subtracted magnetization is much sharper. This confirms that there is a canting in the manganese sublattice which results in localization of the  $e_g$  electrons. However, the most striking feature is the observation of a metallic state in the compound with  $x = 0.4$  below the spin-glass freezing temperature. This clearly indicates that a ferromagnetic component persists in the spin-glass state which is supported by the neutron diffraction results for similar manganite materials showing spin-glass behaviour [4]. It is interesting to note here that if one applies the same criterion as the one used to determine  $T_c$  for the compositions  $x = 0.05$  to 0.3, namely, the maximum of the second derivative of the  $M$ – $T$  curve, one gets  $T_c \sim 104$  K for the  $x = 0.4$  sample from the FC  $M$ – $T$  data at 100 Oe. This correlates very well with the metal–insulator transition temperature of the material. The electrical behaviour of the material will depend on whether the ferromagnetic component in the material exceeds the percolation threshold. The observed metallicity in the spin-glass state thus suggests that for the composition with  $x = 0.4$  the ferromagnetic component in the material is above the percolation threshold.

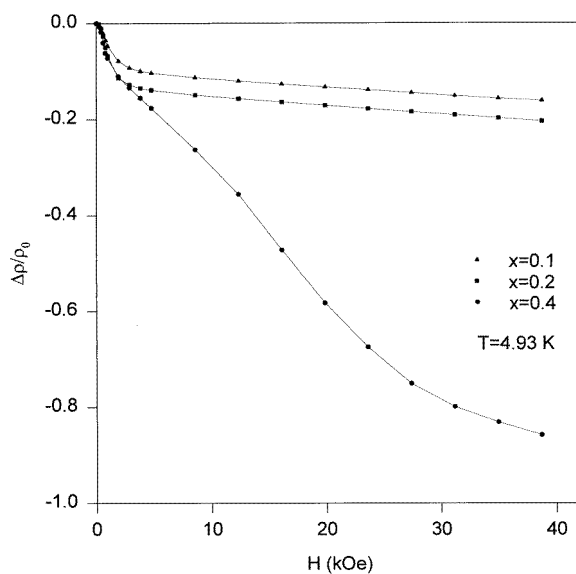


**Figure 7.** The magnetoresistance ratio  $\Delta\rho/\rho_0 \sim (\rho(H) - \rho(H = 0))/\rho(H = 0)$  up to 40 kOe for  $x = 0.1$ ,  $x = 0.2$  and  $x = 0.4$ .

Figure 7 shows the magnetoresistance ( $\Delta\rho/\rho_0 \sim (\rho(H) - \rho(H = 0))/\rho(H = 0)$ ) as a function of field up to 40 kOe for the samples with  $x = 0.1$ , 0.2 and 0.4 at 4.9 K. The magnetoresistance in the spin-glass state ( $x = 0.4$ ) is much larger than for the ferromagnetic compositions  $x = 0.1$  and 0.2. This is understandable since in the ferromagnetic phase the manganese ions are almost fully aligned and the magnetoresistance comes from suppression of domain wall scattering at low fields and suppression of ferromagnetic fluctuations at high

fields. However, in the spin-glass phase application of an external magnetic field results in the suppression of the spin disorder inside the material. This results in a significant decrease in the resistance under a magnetic field.

#### 4. Conclusions

We have studied the systematic evolution of magnetic and transport properties with doping of the smaller rare-earth ion  $\text{Ho}^{3+}$  in  $\text{La}_{0.7}\text{Sr}_{0.3}\text{MnO}_3$ . There is an increasing thermomagnetic irreversibility with holmium doping for  $x \geq 0.2$  leading to a metallic spin-glass-like state for  $x = 0.4$ . In this context it might be mentioned that there is not yet any clear theoretical explanation of how the competition between the ferromagnetic double exchange and antiferromagnetic superexchange can lead to a spin-glass state. On the basis of considerations of superexchange and double exchange only, de Gennes [10] had predicted that the system at low temperature should have a canted antiferromagnetic structure. However, de Gennes' model was a quasi-continuum model in which the positional disorder of  $\text{Mn}^{3+}$  and  $\text{Mn}^{4+}$  was averaged out. It would be interesting to investigate how this site or bond disorder affects the magnetic structure in these materials. We believe that systematic studies of small rare-earth doping in these materials with microscopic probes like neutron diffraction will reveal more about the evolution of the spin-glass phase.

#### References

- [1] Fontcuberta J, Martinez B, Seffar A, Pinol S, Garcia-Munoz J L and Obradors X 1996 *Phys. Rev. Lett.* **76** 1122
- [2] Maignan A, Simon Ch, Caignaert V and Raveau B 1996 *Z. Phys. B* **99** 305
- [3] De Teresa J M, Ibarra M R, Garcia J, Blasco J, Ritter C, Algarabel P A, Marquina C and del Moral A 1996 *Phys. Rev. Lett.* **76** 3392
- [4] Maignan A, Varadaraju U V, Millange F and Raveau B 1997 *J. Magn. Magn. Mater.* **168** L237
- [5] Sundaresan A, Maignan A and Raveau B 1997 *Phys. Rev. B* **55** 5596
- [6] Jirak Z, Krupicka S, Simsa Z, Dlouha M and Vratislav S 1985 *J. Magn. Magn. Mater.* **53** 135
- [7] Yoshizawa H, Kawano H, Tomioka Y and Tokura Y 1995 *Phys. Rev. B* **52** 13 145
- [8] Zener C 1951 *Phys. Rev.* **82** 403
- [9] Morgownik A F J and Mydosh J A 1981 *Phys. Rev. B* **24** 5277  
and see also  
Mydosh J A 1993 *Spin Glasses: An Experimental Introduction* (London: Taylor & Francis)
- [10] de Gennes P G 1960 *Phys. Rev.* **118** 141